Cell, Vol. 109, 61–73, April 5, 2002, Copyright ©2002 by Cell Press

The bHLH Transcription Factors OLIG2 and OLIG1 Couple Neuronal and Glial Subtype Specification

Qiao Zhou[1] and David J. Anderson[1,2,3]
[1]Division of Biology 216-76
[2]Howard Hughes Medical Institute
California Institute of Technology
Pasadena, California 91125

Summary

OLIG1 and OLIG2 are basic-helix-loop-helix (bHLH) transcription factors expressed in the pMN domain of the spinal cord, which sequentially generates motoneurons and oligodendrocytes. In *Olig1/2* double-mutant mice, motoneurons are largely eliminated, and oligodendrocyte differentiation is abolished. Lineage tracing data suggest that *Olig1*$^{-/-}$*2*$^{-/-}$ pMN progenitors instead generate V2 interneurons and then astrocytes. This apparent conversion likely reflects independent roles for OLIG1/2 in specifying motoneuron and oligodendrocyte fates. *Olig* genes therefore couple neuronal and glial subtype specification, unlike proneural bHLH factors that control the neuron versus glia decision. Our results suggest that in the spinal cord, *Olig* and proneural genes comprise a combinatorial code for the specification of neurons, astrocytes, and oligodendrocytes, the three fundamental cell types of the central nervous system.

Introduction

The three fundamental cell types of the vertebrate central nervous system (CNS) are neurons, astrocytes, and oligodendrocytes. This basic triad comprises many hundreds or even thousands of distinct neuronal subtypes, in addition to subtypes of astroglia and perhaps of oligodendroglia as well (Raff, 1989; Woodruff et al., 2001). The molecular mechanisms by which these diverse neural cell types are properly generated in space and time are incompletely understood. In recent years, a great deal has been learned about the transcriptional control of the neuron-glial fate decision (Tomita et al., 2000; Nieto et al., 2001; reviewed in Vetter, 2001) and about the control of neuron subtype specification (Briscoe et al., 2000; Jessell, 2000). Rather less is known, however, about the transcriptional control of glial subtype determination.

Two major classes of transcription factors have emerged as determinants of neuron versus glial fate determination and of neuron subtype specification: the basic-helix-loop-helix (bHLH) factors (Vetter, 2001) and homeodomain (HD) factors (Jessell, 2000), respectively. In vertebrates, bHLH factors homologous to the *Drosophila* proneural genes, such as the *Neurogenins (Ngns)* (Gradwohl et al., 1996; Ma et al., 1996; McCormick et al., 1996) and *Mash1* (Johnson et al., 1990), promote neuronal differentiation at the expense of the glial fate (Tomita et al., 2000; Nieto et al., 2001; Sun et al., 2001b). In the spinal cord, a combinatorial code of HD transcription factors specifies the regional identity of progenitor domains along the dorso-ventral axis (Briscoe et al., 2000; Jessell, 2000). Motoneurons are generated from the pMN domain, while V0, V1, V2, and V3 interneurons are generated from the p0, p1, p2, and p3 domains, respectively (Briscoe et al., 2000; Jessell, 2000). This discontinuous patterning arises from mutually repressive interactions between the HD factors that specify adjacent progenitor domains (Briscoe et al., 2000; Muhr et al., 2001).

Recently, we and others identified a subclass of neural bHLH factors, called *Olig* genes (Lu et al., 2000; Takebayashi et al., 2000; Zhou et al., 2000). In the mouse, there are two *Olig* genes that are specifically expressed in oligodendrocyte precursors, called *Olig1* and *2* (Lu et al., 2000; Zhou et al., 2000), while in the chick a single gene orthologous to *Olig2* has been identified (Mizuguchi et al., 2001; Zhou et al., 2001). In the spinal cord, oligodendrocyte precursors emerge from a highly restricted domain of the ventral ventricular zone (Miller, 1996; Richardson et al., 2000). This region is precisely demarcated by expression of *Olig1* and *Olig2* (Lu et al., 2000; Zhou et al., 2000). *Olig2* is sufficient to cause ectopic differentiation of oligodendrocytes in the chick spinal cord when misexpressed together with the HD factor Nkx2.2 (Sun et al., 2001a; Zhou et al., 2001), while *Olig1* promotes oligodendrocyte differentiation in rodent cortex (Lu et al., 2001).

Prior to oligodendrogliogenesis, the domain of *Olig2* expression corresponds to the pMN domain, from which motoneurons are generated (Takebayashi et al., 2000; Mizuguchi et al., 2001; Novitch et al., 2001). Gain-of-function experiments suggest that OLIG2 plays a determinative role in patterning the pMN domain and also initiates motoneuron differentiation and cell cycle arrest, in part by promoting expression of *Ngn2* (Mizuguchi et al., 2001; Novitch et al., 2001). These data suggest that OLIG2 sequentially controls both motoneuron and oligodendrocyte fate determination. Interestingly, the bHLH factor appears to function in both cases as a transcriptional repressor (Novitch et al., 2001; Zhou et al., 2001).

To rigorously assess the requirement for *Olig* genes in motoneuron and oligodendrocyte differentiation, we have generated double-homozygous mice lacking both *Olig1* and *Olig2*. In *Olig1/2* double mutants, presumptive motoneuron precursors are transformed into V2 interneuron precursors, and oligodendrocytes are lost throughout the brain and spinal cord. Surprisingly, many *Olig2*-expressing oligodendrocyte precursors are transformed into astrocytes. Thus, in the absence of *Olig1/2* function, the sequential production of motoneurons and oligodendrocytes is converted into the sequential production of interneurons and astrocytes. These data suggest that *Olig* genes couple neuronal and glial subtype specification.

Results

Generation of *Olig1* and *Olig2* Double-Mutant Mice

The coexpression of *Olig1* and *Olig2* in vivo (Zhou et al., 2000) raised the possibility that deletion of either of

[3]Correspondence: wuwei@caltech.edu

these genes alone might be compensated by the function of the other. In order to circumvent this problem, we decided to generate an *Olig1* and *Olig2* double mutant. The mouse *Olig1* and *Olig2* genes are tightly linked on chromosome 16, about 36 kb from each other (data not shown). In order to preserve the *Olig1-Olig2* intergenic region, double-mutant mice were generated through two rounds of homologous recombination in ES cells. The *Olig2* coding region was replaced by a targeting cassette composed of a histone-GFP (hGFP) fusion (Kanda et al., 1998) and PGK-neomycin (Figures 1A and 1B), while the *Olig1* coding region was replaced by a tau-LacZ and PGK-hygromycin cassette (Figures 1D and 1E).

Using a Cre/lox-mediated analytic strategy (see Experimental Procedures), two ES clones were identified in which the *Olig1* and *Olig2* targeted loci lay in *cis* (Figure 1H). Sister cells from these clones, unmodified by Cre recombinase, were injected into blastocysts, and the targeted alleles were transmitted through the germ line (Figures 1C and 1F). Double-heterozygous mice were born at the expected Mendelian frequency and were viable and fertile. However, no live births of homozygous mice were observed, and starting from E18.5, the homozygous embryos appeared smaller than their littermates.

We initially examined the pattern of GFP and LacZ expression in heterozygous *Olig1*$^{+/-}$*Olig2*$^{+/-}$ embryos between E9.5 and E16.5. At E9.5, GFP was strongly expressed in a ventral domain of the spinal cord that corresponds to pMN (Figure 1I), similar to the pattern of endogenous *Olig2* expression (Figure 1J; also see Takebayashi et al., 2000). In contrast, only a few cells were observed to be weakly lacZ positive at this stage (Figure 1N), in agreement with the relatively weak expression of endogenous *Olig1* during the period of neurogenesis (Figure 1O). At E16.0, when *Olig2* expression is restricted to oligodendrocyte precursors (Lu et al., 2000; Zhou et al., 2000), nearly all OLIG2-positive cells were also GFP-positive (Figures 1K–1M, arrows). In addition, GFP colocalized extensively with the *Olig1* knockin marker tau-lacZ (Figures 1P–1R, arrows), consistent with the coexpression of endogenous *Olig1* and *2* in oligodendrocyte precursors (Zhou et al., 2000). Thus, in heterozygous *Olig1*$^{+/-}$*Olig2*$^{+/-}$ mice, the expression of GFP and tau-lacZ faithfully recapitulates the pattern of endogenous *Olig2* and *Olig1* expression in cells of both the motoneuron and oligodendrocyte lineages.

Deletion of *Olig2* and *Olig1* Results in Loss of Motoneurons and a Concomitant Ventral Expansion of V2 Interneurons

We first focused our analysis of *Olig1/2* double-mutant embryos on the generation of several neuronal subtypes derived from the four ventral-most progenitor domains of the spinal cord: En1$^+$ V1 interneurons, Chx10$^+$ V2 interneurons, Isl1/2$^+$ and Hb9$^+$ motoneurons, and Ngn3$^+$ V3 interneurons (Figures 2A–2E). Most Isl1/2$^+$, Hb9$^+$ motoneurons were lost at all axial levels of the homozygous mutant spinal cord at E10.5 (Figures 2H, 2I, and 2K, white bars), while the number of such motoneurons was the same in heterozygote and wild-type (Figures 2C, 2D, and 2K, dark and light gray bars). The loss of motoneurons in the *Olig1*$^{-/-}$*Olig2*$^{-/-}$ spinal cord was not due to cell death, as no increased apoptosis was detected by the TUNEL assay at this stage (Figures 3O and 3T). Although very few presumptive motoneurons (Isl1/2$^+$, Hb9$^+$ cells) were detectable at E10.5 in *Olig1*$^{-/-}$*Olig2*$^{-/-}$ embryos (Figures 2H and 2I, arrowheads), it was possible that a normal number of these neurons might be recovered at later stages through compensatory mechanisms. However, at E13.5, neither somatic (Figures 2L and 2M, arrows) nor visceral (Figures 2L and 2M, arrowheads) motoneurons were detected in the *Olig1*$^{-/-}$*Olig2*$^{-/-}$ spinal cord (Figures 2P and 2Q, arrows and arrowheads, and 2T, white bars). Moreover, no projecting axons were observed in the ventral root (Figures 2O and 2S, arrows), consistent with a lack of both classes of spinal motoneurons.

In contrast to the dramatic loss of motoneurons, the number of Chx10$^+$ cells, which derive from the p2 domain just dorsal to the pMN domain, was increased by about 80% in the double-null mutant spinal cord at E10.5 (Figures 2B versus 2G; 2K, Chx10, white bar). Furthermore, many Chx10$^+$ cells occupied a more ventral position, in territory normally occupied by motoneurons (Figure 2G, yellow arrowhead). The increased number and ventral expansion of Chx10$^+$ V2 interneurons were also apparent at E13.5 (Figures 2N, 2R, and 2T). The number and distribution of En1$^+$ V1 interneurons and Ngn3$^+$ V3 interneurons, by contrast, were largely unaltered in the mutant (Figures 2A, 2E, 2F, 2J, and 2K).

The preceding data suggested that in the absence of *Olig1/2* function, pMN progenitors might give rise to V2 interneurons instead of motoneurons. To confirm this, we used the *Olig2* knockin marker hGFP as a short-term lineage tracer to compare the identities of the neuronal progeny derived from the pMN domain of heterozygous versus homozygous *Olig1/2* double-mutant embryos. In heterozygotes, *Olig2-hGFP*-derived precursors gave rise to Islet1/2$^+$ motoneurons (Figure 3A, yellow cells) but not Chx10$^+$ V2 interneurons (Figure 3B). By contrast, in the homozygotes there were many GFP$^+$, Chx10$^+$ cells present in the marginal zone lateral to the pMN domain of the ventricular zone (Figure 3G, yellow cells). At no time did we detect any Islet1/2$^+$Chx10$^+$ phenotypically hybrid cells (data not shown). In the immediately overlying p2 domain, Chx10$^+$GFP$^-$ V2 interneurons were produced in both heterozygotes and homozygotes (Figures 3B and 3G, white arrowheads). These data strongly suggest that precursor cells from the pMN domain of *Olig1/2* homozygous animals generate V2 interneurons instead of motoneurons.

Irx3 Is Derepressed in pMN in the Absence of *Olig2* and *Olig1* and Respecifies pMN to p2

The loss of motoneurons and concomitant ventral expansion of V2 interneurons in the double-null mutant could reflect a conversion of the pMN domain to a p2 identity. Consistent with this idea, the expression of Irx3, a p2 domain patterning molecule (Briscoe et al., 2000), expanded into the pMN domain in *Olig1*$^{-/-}$*Olig2*$^{-/-}$ double mutants at E10.5 (Figures 3C and 3H, arrows). Pax6 expression, which is high in the p2 domain but lower in the pMN domain (Figures 3D, arrow, and 3E), also

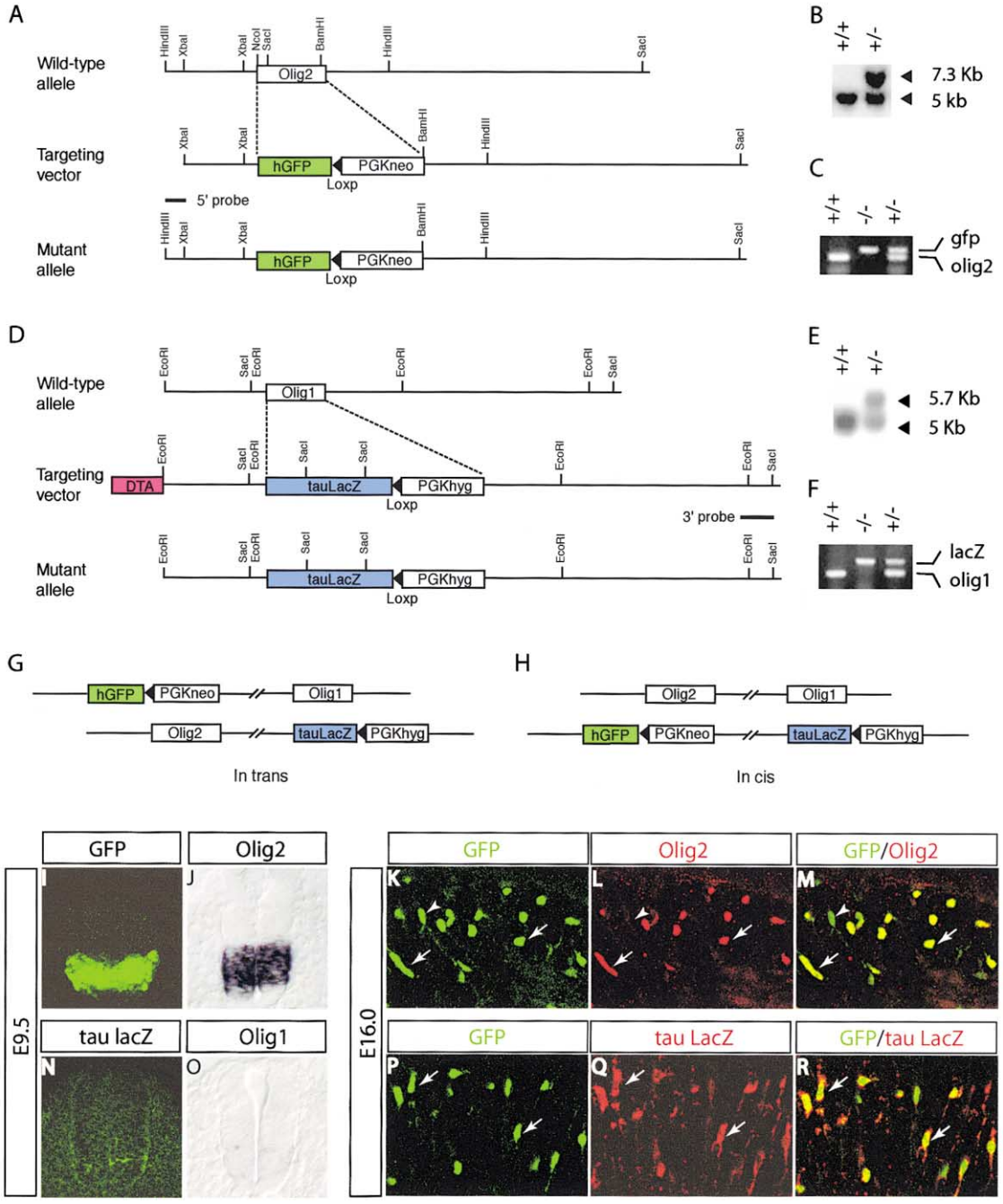

Figure 1. Inactivation of *Olig1* and *Olig2* by Homologous Recombination

(A–C) First round of homologous recombination at the *Olig2* locus.

(A) A *Histone-EGFP/loxp/PGK* neomycin cassette replaced the *Olig2* coding region.

(B) Correct recombination at *Olig2* locus verified by Southern blot analysis of ES clones.

(D–F) Second round of homologous recombination at the *Olig1* locus.

(D) A *tau-LacZ/loxp/PGK* hygromycin cassette replaced the *Olig1* coding region in ES cells in which one *Olig2* locus had been successfully targeted. Abbreviation: DTA, diphtheria toxin A chain.

(E) Correct recombination at the *Olig1* locus verified by Southern blot.

(C and F) Successful germline transmission of the targeted *Olig2* and *Olig1* alleles in *Olig1,2* double-mutant embryos confirmed by genotyping with specific PCR primers.

(G and H) Schematic diagram showing that the two targeting cassettes could lie either in *trans* (G) or in *cis* (H) to each other. A Cre/Loxp analysis was used to identify ES cells in which the two cassettes lie in *cis* (see Experimental Procedures).

(I, J, N, and O) Expression of histone-EGFP and tau-LacZ in the heterozygotes. Thoracic spinal cord sections of E9.5 *Olig1*$^{+/-}$*Olig2*$^{+/-}$ heterozygous embryos were either labeled with anti-GFP antibody (I) or anti-LacZ antibody (N) or were probed by in situ hybridization with cRNAs against Olig2 (J) and Olig1 (O).

(K–M and P–R) Thoracic spinal cord sections from E16.0 *Olig1*$^{+/-}$*Olig2*$^{+/-}$ heterozygous embryos were double labeled with antibodies to GFP and Olig2 (K–M) or to GFP and lacZ (P–R). Extensive colocalization of GFP and Olig2 (K–M) as well as GFP and tau LacZ (P–R) were observed. Arrows indicate double-positive cells. A small number of GFP^{+} cells was found to be Olig2^{-} at this stage (K–M, arrowheads).

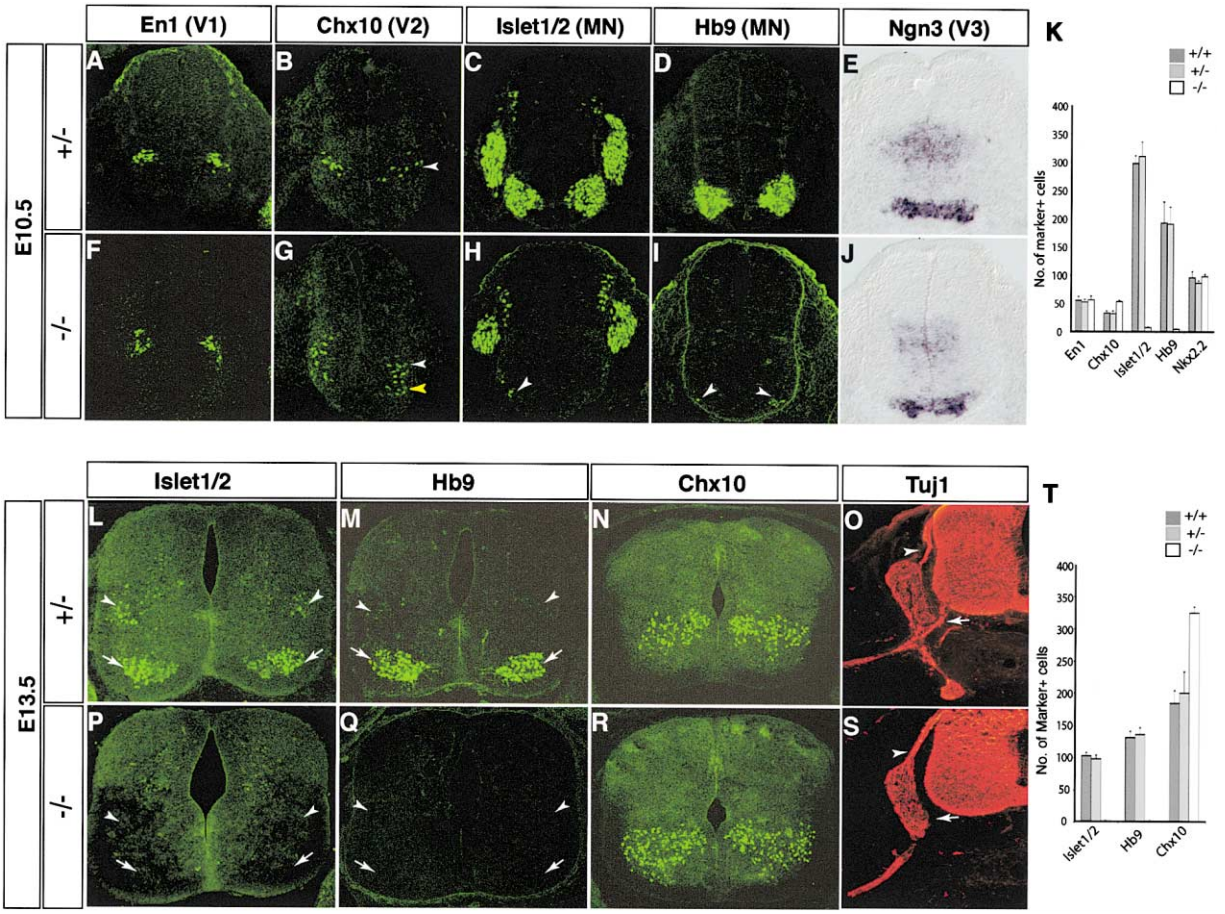

Figure 2. Loss of Isl1/2$^+$Hb9$^+$ Motoneurons and Concomitant Ventral Expansion of Chx10$^+$ V2 Interneurons in the Absence of *Olig1* and *Olig2*

(A–K) Crosssections of E10.5 thoracic spinal cord were stained with antibodies to detect four types of ventral neurons: En1$^+$ V1 interneurons (A and F), Chx10$^+$ V2 interneurons (B and G, arrowheads), Isl1/2$^+$ and Hb9$^+$ motoneurons (C, D, H, and I), and Ngn3$^+$ V3 interneurons (E and J). Note the dramatic reduction of Isl1/2$^+$ and Hb9$^+$ motoneurons in the homozygous spinal cord (C, D, H, and I), while the Chx10$^+$ V2 neurons increased in number and expanded ventrally (B and G, arrowheads). Arrowheads in (H) and (I) indicate the few residual motoneurons formed in the homozygote. White and yellow arrowheads in (B) and (G) indicate Chx10$^+$ V2 interneurons in the p2 and pMN domains, respectively. Quantitative analysis is shown in (K). The number of marker positive cells is presented as mean ± S.D. from nine sections of three embryos. Isl1/2$^+$Hb9$^+$ motoneurons decreased to <5%, and Chx10$^+$ V2 neurons increased ~80% in the double-null mutant compared to heterozygote or wild-type.

(L–T) Motoneuron phenotype at E13.5. Both visceral (L and M, arrowheads) and somatic (L and M, arrows) motoneurons were lost in the homozygotes (P and Q, arrowheads and arrows). In addition, projecting axons were selectively lost in the ventral root of the null mutant (O and S, arrows). Quantitative analysis revealed a 60% increase in the number of Chx10$^+$ cells in the double-null mutant (T; mean ± S.D., six sections from 2–3 animals).

increased in the pMN domain of the null mutant, so that cells in both pMN and p2 were now expressing equally high levels of Pax6 (Figure 3I, arrow). The observed ventral expansion of Irx3 is predicted by the observation that Irx3 and OLIG2 exert crossrepressive activities in gain-of-function assays (Novitch et al., 2001). Surprisingly, however, it did not cause a complete loss of GFP expression from the *Olig2* locus (Figures 3P and 3R), perhaps because the repressive effect of Irx3 is overridden by the higher levels of Shh signaling more ventrally. The expression of several other ventral spinal cord patterning molecules, including Dbx2, Nkx6.1, Nkx6.2, and Nkx2.2 (Briscoe et al., 2000), was unchanged in *Olig1/2* double mutants (data not shown). Taken together, these data suggest that in the absence of *Olig1/2*, pMN cells are converted to a p2 identity (Figures 3E and 3J).

Olig2 and *Olig1* Regulate Neurogenin 2 Expression in pMN

Ectopic expression studies in chick suggested that deletion of *Olig2* and *Olig1* should cause a loss of *Ngn2* expression in the pMN domain (Novitch et al., 2001). Consistent with this prediction, no NGN2-positive cells were detected in the presumptive pMN domain of the *Olig1*$^{-/-}$*Olig2*$^{-/-}$ mutant at E10.0 (Figure 3P), while prominent NGN2 expression was evident in the GFP$^+$ pMN domain of the heterozygous spinal cord (Figure 3K, yellow cells). The lack of apoptotic cells detected by TUNEL labeling in the mutant spinal cord (Figures 3O and 3T) suggests that the loss of NGN2$^+$ cells in the pMN domain does not reflect cell death. We also observed a slight ventral expansion of MASH1 into pMN in *Olig1/2* double mutants (Figures 3L versus 3Q, arrow).

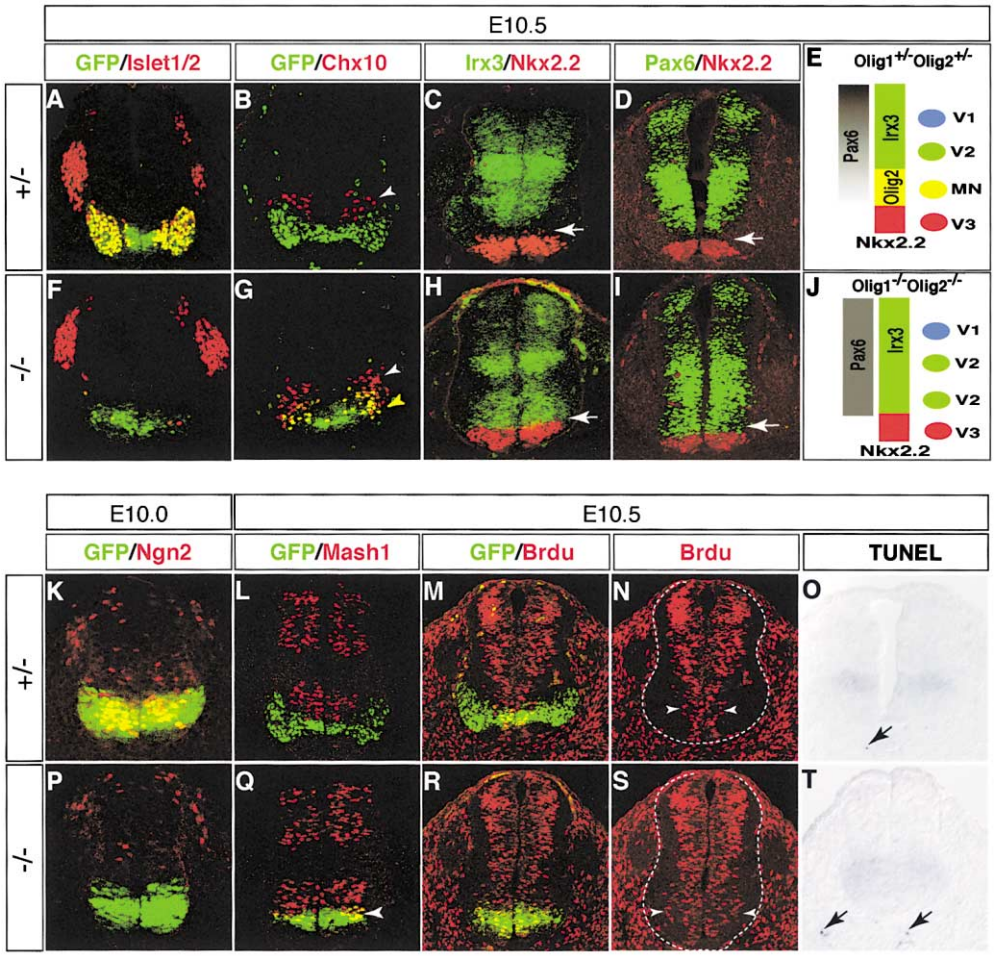

Figure 3. Derepression of *Irx3* and Repression of *Neurogenin2* in the pMN Domain of *Olig1*$^{-/-}$*Olig2*$^{-/-}$ Embryos

(A, B, F, and G) OLIG2-hGFP^{+} precursors in pMN generate Islet1/2^{+} motoneurons in heterozygotes (A, yellow cells) but instead produce Chx10^{+} V2 interneurons in homozygotes (G, yellow arrowhead). White arrowheads in (B) and (G) indicate Chx10^{+}, OLIG2-hGFP^{-} V2 interneurons generated from the p2 domain.

(C and H) Irx3 is derepressed in the pMN of the mutant spinal cord (H, arrow), as is Pax6 (D and I; arrows indicate pMN domain).

(E and J) Summary of the ventral spinal cord patterning defects in *Olig1/2* mutants.

(K, P) Neurogenin 2 (Ngn2) expression is selectively lost in pMN of the mutant at E10.0, while a delayed expansion of MASH1 into this domain is detected at E10.5 (L and Q, arrowhead).

(M, N, R, and S) Many BrdU^{+} cells persist outside the ventricular zone of the pMN in the null mutant (S, arrowheads) compared to heterozygotes (N); the same fields with GFP expression superimposed are shown in (R) and (M), respectively.

(O and T) No significant cell death was observed in the spinal cord at this stage (E10.5). Arrows indicate apoptotic cells outside the spinal cord.

As *Mash1* has recently been shown to be necessary and sufficient for Chx10 expression (Parras et al., 2002), these results may explain how V2 interneurons can differentiate from the mutant pMN despite the absence of NGN2 (Scardigli et al., 2001).

Since NGN2 has been shown to promote cell cycle exit and terminal differentiation (Farah et al., 2000; Novitch et al., 2001), we reasoned that the loss of *Ngn2* expression in pMN might cause delayed cell cycle exit by pMN-derived precursors as they migrated from the ventricular zone. To assess this, we measured BrdU incorporation after a 2 hr pulse in vivo at E10.5. An increased number of BrdU^{+} cells was detected outside the ventricular zone in the GFP^{+} region of the double-null mutant (Figures 3M, 3N, 3R, and 3S, arrowheads). These data suggest that pMN cells lacking OLIG2 fail to exit the cell cycle before migrating into the marginal zone. The presence of ectopic MASH1^{+} cells in pMN is not inconsistent with this observation, as we have recently found that MASH1 promotes cell cycle arrest less efficiently than does NGN2 (Lo et al., 2002).

Failure of Oligodendrocyte Development in *Olig1/2* Double Mutants

We next examined the phenotypic consequences of *Olig2* and *Olig1* deletion on the development of oligodendrocytes. To detect oligodendrocyte precursors, *PDGFR*α and *Sox10* were used as markers (Hall et al., 1996; Zhou et al., 2000), while *MBP* and *PLP/DM20* were used to detect mature oligodendrocytes (Zhou et al., 2001). At no time did we detect expression of any of these markers in the *Olig1/2* double-homozygous mutant at all axial levels of spinal cord examined (Figure 4, $-/-$, and data not shown) as well as in all brain

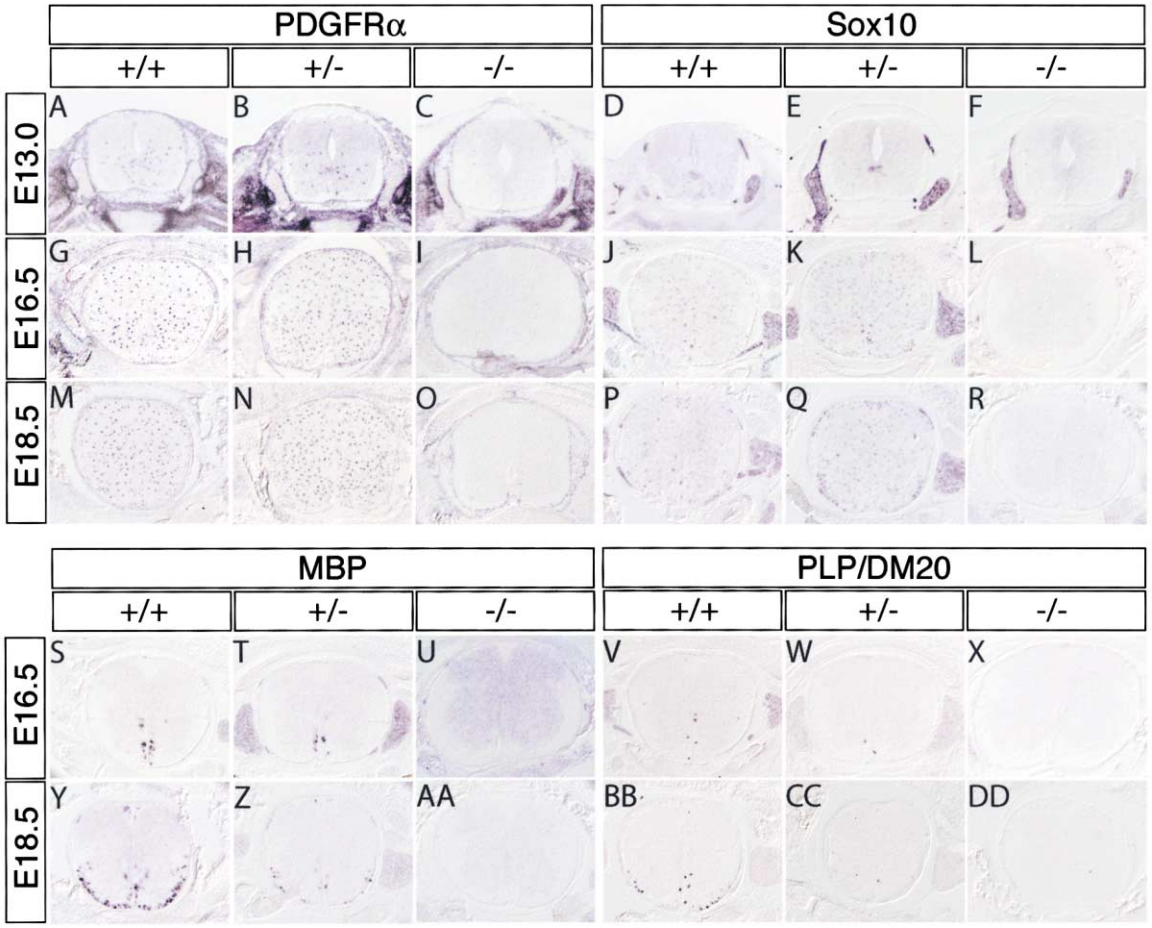

Figure 4. Spinal Cord Oligodendrocytes Fail to Develop in the Absence of *Olig1* and *Olig2*

(A–R) In situ hybridization with the oligodendrocyte precursor markers *PDGFRα* and *Sox10* on crosssections of thoracic spinal cord at indicated stages. Note the total absence of *PDGFRα* and *Sox10* expression in the null mutant spinal cord (C, F, I, L, O, and R).

(S–DD) No *MBP*$^+$ or *PLP/DM20*$^+$ mature oligodendrocytes were detected in null mutant spinal cord (U, X, AA, and DD). In addition, the number of *MBP*$^+$ and *PLP/DM20*$^+$ oligodendrocytes was smaller in the heterozygotes (Z and CC) than in wild-type (Y and BB) at E18.5.

areas examined (Figures 5D–5F and data not shown). In contrast, numerous cells expressing these oligodendrocyte precursor and differentiation markers were present in the wild-type (Figure 4, +/+) and heterozygous (Figure 4, +/−) spinal cord and brain (Figures 5A–5C and data not shown). Thus, there is a total failure of oligodendrocyte formation in the *Olig1*$^{-/-}$*Olig2*$^{-/-}$ double mutant.

Cell counts at E16.5 revealed no decrease in the number of *PDGFRα*$^+$ precursors at thoracic levels of the spinal cord in heterozygotes compared to wild-type (297 ± 17 versus 290 ± 19 cells per 18 μm section, respectively; mean ± S.D., n = 6 sections from three embryos). Consistent with these data, in heterozygotes at E16.5 and P8, *MBP* and *PLP/DM20* expression was normal (Figures 4S, 4T, 4V, and 4W and data not shown). Surprisingly, however, between E18.5 and P0, there was significantly less expression of these mature oligodendrocyte markers in the heterozygotes compared to wild-type (Figures 4Y, 4Z, 4BB, and 4CC and data not shown). These data suggest that a full dosage of *Olig* genes is required for the progression of oligodendrocyte differentiation but not for the initiation of this process.

Olig1 Is Functionally Redundant with *Olig2* in Hindbrain Oligodendrocyte Development

We next examined the phenotype of *Olig1/2* double-knockout embryos in the hindbrain. As in the spinal cord, hindbrain somatic motoneuron differentiation did not occur in *Olig1/2* double mutants, as evidenced by the loss of Isl1/2$^+$, Hb9$^+$ cells and of the XIIth cranial somatic motor nerve (Figures 5G–5I versus 5J–5L, arrows). In contrast, visceral motoneurons, identified by coexpression of Isl1/2 and Phox2b (Dubreuil et al., 2000), were generated (Figures 5J–5L, arrowheads). These results are consistent with the fact that visceral motoneurons in the hindbrain derive from the p3 domain (Briscoe et al., 1999), which does not express either *Olig1* or *Olig2* (data not shown).

In *Olig2*$^{-/-}$ single mutants, oligodendrocytes are spared in the hindbrain while they are lost throughout the spinal cord (Lu et al., 2002 [this issue of *Cell*]). In contrast, we found that neither oligodendrocyte precursors nor mature oligodendrocytes were generated in the hindbrain of *Olig1/2* double mutants (Figures 5D–5F), as was the case in all other brain areas examined (not shown). Taken together, these data suggest that *Olig1*

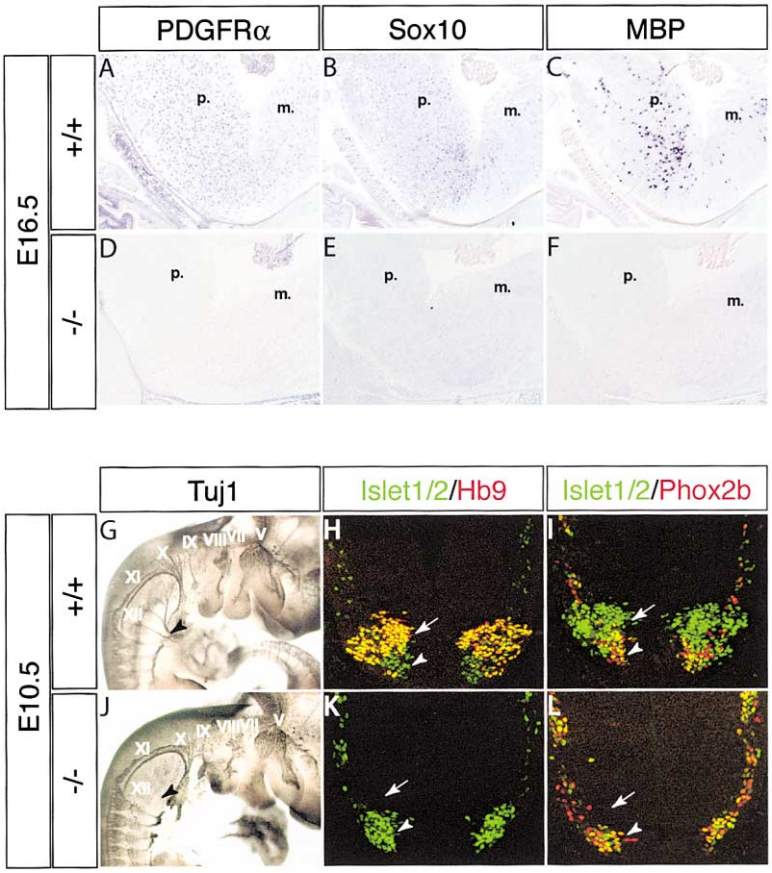

Figure 5. Loss of Hindbrain Oligodendrocytes in the Null Mutant Is Preceded by the Loss of Hindbrain Somatic But Not Visceral Motoneurons

(A–F) In situ hybridization was performed on head saggital sections of E16.5 wild-type or double-null mutant embryos. The pictures were taken from the midbrain-hindbrain region encompassing pons (p.) and medulla (m.). No oligodendrocytes were present in the hindbrain (D–F) as well as other brain areas of the double mutants (data not shown).

(G and J) Whole-mount Tuj1 antibody labeling of E10.5 embryos. The XIIth cranial motor nerve (hypoglossal, arrowhead) was missing from the homozygote.

(H–L) In the caudal hindbrain of the null mutant, Isl1/2^{+} and Hb9^{+} somatic motoneurons were lost (K and L, arrows), while Isl1/2^{+} and Hb9^{-} visceral motoneurons were still present (K and L, arrowheads).

can compensate for the lack of *Olig2* in oligodendrocyte (but not somatic motoneuron) generation in the hindbrain but not in other regions of the CNS.

Oligodendrocyte Precursors Are Transformed into Astrocytes in the Absence of *Olig2* and *Olig1*

The absence of oligodendrocyte precursors in *Olig1/2* double-mutant embryos could reflect a failure of specification, their death, or their respecification into other cell types. To distinguish between these possibilities, we first tested whether there was increased cell death in the *Olig1*$^{-/-}$*Olig2*$^{-/-}$ spinal cord from E12 to E14, a period when oligodendrocyte precursors are specified in the ventricular zone. TUNEL labeling detected no increase in apoptotic cells in either the ventricular zone or elsewhere in the spinal cord during this interval (data not shown). Next, we used the knockin marker hGFP as a short-term lineage tracer to compare the fate of *Olig2*-expressing progenitors in the presence or absence of *Olig1/2* function.

In heterozygous embryos at E13.5, individual GFP^{+} precursors could be seen migrating away from the focus of *Olig2* expression in the ventricular zone (Figure 6A, arrow and white arrowheads). By E16.5, only a few GFP^{+} cells remained at this focus (Figure 6B, arrow), and most had migrated into the gray matter. By E18.5, GFP^{+} oligodendrocyte precursors were evenly distributed throughout the spinal cord, and ventricular expression was no longer detected (Figure 6C). The pattern of migration of GFP^{+} cells in the heterozygous spinal cord closely resembles that revealed by antibody staining for endogenous OLIG2 protein (Figures 1I–1K, arrows and data not shown).

In homozygous mutant embryos, the distribution of GFP^{+} cells was different in several respects. First, although many GFP^{+} cells were present in the ventricular zone at E13.5 (Figure 6D, arrow), there was little migration into the gray matter. Second, the ventricular focus of GFP expression appeared larger in homozygous than in heterozygous embryos (Figures 6A versus 6D, arrows). Cell counts indicated a similar number of GFP-expressing cells in the null mutant versus heterozygous spinal cord at this stage (Figure 6G, E13.5), suggesting that *Olig2*-expressing cells may have been generated in correct numbers in the homozygote but somehow failed to migrate on schedule. At E16.5 and E18.5, however, there was a reduction in the number of GFP^{+} cells in the double mutant (Figure 6G, white bars). This difference likely reflects reduced proliferation rather than death, as TUNEL labeling revealed no differences between the double mutant and heterozygote at these stages (data not shown).

By E16.5, although ventricular expression of GFP in homozygotes persisted (Figure 6E, arrow), GFP^{+} cells could be seen migrating into the gray matter (Figure 6E, arrowheads). However, these cells took a more ventral trajectory than in heterozygotes. At E18.5, many GFP^{+} cells could be detected at the pial surface of the ventral white matter in homozygotes (Figure 6F, open arrowheads), a location not occupied by GFP^{+} cells in hetero-

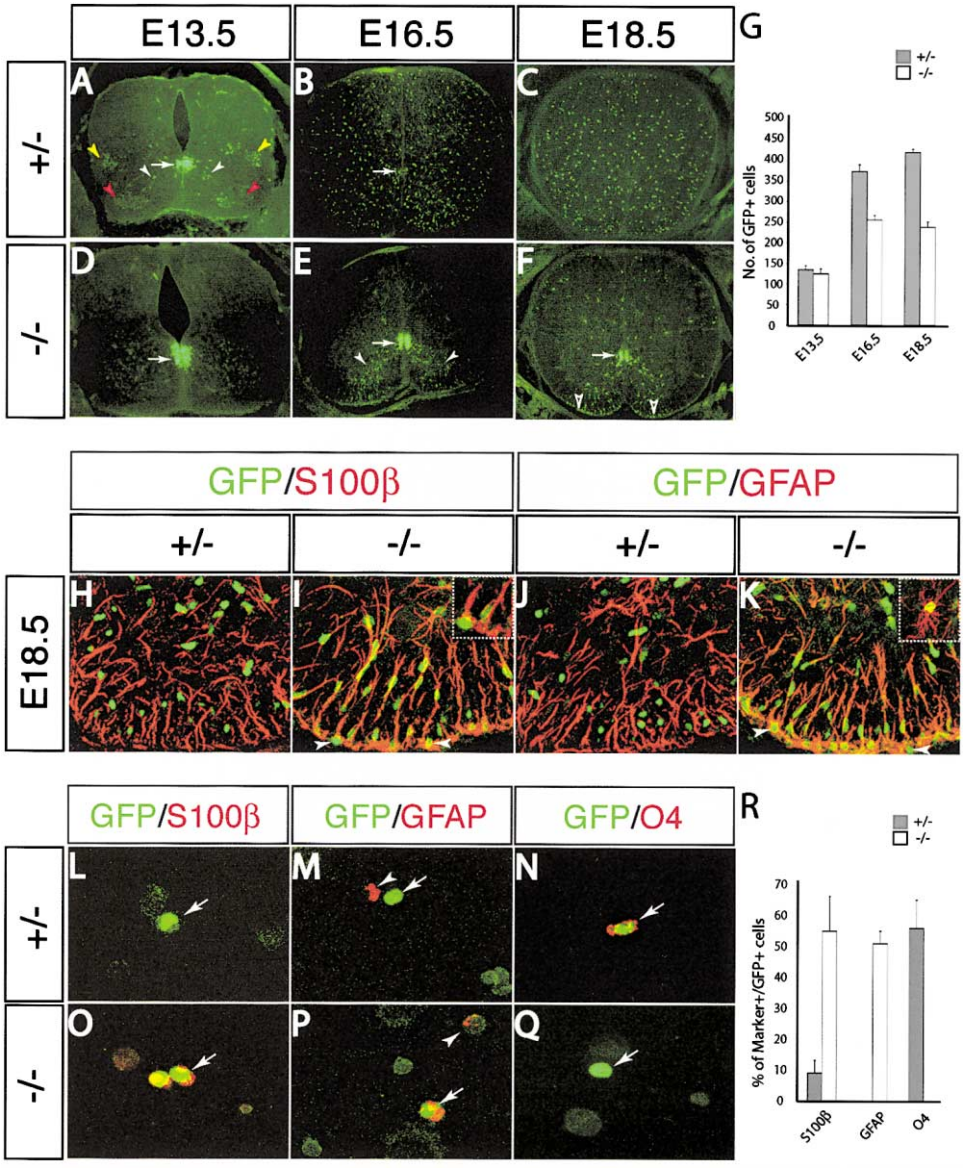

Figure 6. Oligodendrocytes Are Transformed into Astrocytes in the Absence of *Olig1* and *Olig2*

(A–G) Crosssections of heterozygous and homozygous thoracic spinal cord at indicated stages were labeled with an anti-GFP antibody. Arrows indicate ventricular expression of GFP. Persistence of GFP was apparent in both somatic (A, red arrowheads) and visceral (A, yellow arrowheads) motoneurons in the heterozygotes at E13.5, a time when the migration of GFP^+ oligodendrocyte precursors just started (A, white arrowheads). Open arrows in (F) indicate GFP^+ cells located within pial surface. Quantitative analysis (G; mean ± S.D., eight sections from two embryos) revealed a difference in the number of GFP^+ cells in the null mutants versus heterozygotes at E16.5 and E18.5, but not E13.5. (H–K) Many GFP^+ nuclei are associated closely with $S100\beta^+$or $GFAP^+$ fibers in the ventral spinal cord of homozygotes (I and K) but not of heterozygotes (H and J) at E18.5. Arrows point to GFP^+ cells in the pial surface of the null mutant spinal cord. Inserts in (I) and (K) show double-labeled cells at higher magnification.

(L–R) Staining of acutely dissociated spinal cord cells at E18.5 from either heterozygotes (L–N) or homozygotes (O–Q). Arrows point to GFP^+ cells. Arrowheads in (M) and (P) mark GFP^-GFAP^+ cells. Quantitative analysis (R) was performed by counting all GFP^+ cells from six different preps derived from different animals. Each prep contained ~5000 cells.

zygotes (Figure 6C). This observation suggested that the GFP^+ cells might have been transformed into astrocytes. To address this possibility, crosssections of E18.5 heterozygous or homozygous spinal cord were double labeled with antibodies to GFP and the astroglial markers GFAP or S100β. This analysis revealed that many GFP^+ cells in the null mutant spinal cord coexpressed GFAP or S100β (Figures 6I and 6K, arrowheads and insets). In contrast, no colocalization of GFP with either of these markers was observed in the heterozygous spinal cord (Figures 6H and 6J), consistent with previous reports that *Olig2* is not expressed in cells of the astroglial lineage in wild-type embryos (Lu et al., 2000; Zhou et al., 2000).

The filamentous staining pattern of GFAP and S100β precluded an accurate quantification of the percentage of GFP^+ cells that were $GFAP^+$ or $S100\beta^+$ in vivo. To circumvent this problem, we performed double-labeling on acutely dissociated spinal cord cells from E18.5 heterozygous and homozygous embryos. Over 50% of GFP^+ cells in homozygous spinal cord coexpressed GFAP (Figures 6P, arrow, and 6R, GFAP, white bar). In sharp contrast, none of the GFP^+ cells in the heterozygous spinal cord was found to be $GFAP^+$ (Figures 6M, arrow versus arrowhead, and 6R, gray bars). Similarly, 44% to 66% of GFP^+ cells were $S100\beta^+$ in the homozygote (Figures 6O, arrow, and 6R, white bar), whereas less than 10% of GFP^+ cells in the heterozygote were $S100\beta^+$ (Figures 6L, arrow, and 6R, gray bar). Conversely, the oligodendrocyte cell-surface marker O4 decorated over 55% of GFP^+ cells in the heterozygous spinal cord (Figures 6N, arrow, and 6R, gray bar) but none in the homozygote (Figures 6Q, arrow, and 6R, white bar). The reciprocal change in the percentage of GFP^+ cells expressing O4 versus GFAP or S100β in heterozygous versus double homozygous embryos (Figure 6R) strongly suggests that in the absence of *Olig1/2* function, the *Olig2*-expressing cell population produces astrocytes rather than oligodendrocytes. Consistent with this conclusion, in cultures of neural progenitors from *Olig1/2* homozygous embryonic spinal cord, many Olig2-hGFP-expressing cells differentiated to astrocytes but none differentiated to oligodendrocytes, whereas in cultures from heterozygotes, many GFP^+ oligodendrocytes developed (see Supplemental Figure S1 at http://www.cell.com/cgi/content/full/109/1/61/DC1).

Discussion

The bHLH transcription factors OLIG1 and OLIG2 are sequentially expressed in motoneuron progenitors (Takebayashi et al., 2000; Mizuguchi et al., 2001; Novitch et al., 2001) and oligodendrocyte precursors (Lu et al., 2000; Zhou et al., 2000). Here we show that in the absence of *Olig1* and *2* function, motoneurons are converted to V2 interneurons in the spinal cord, while oligodendrocytes fail to differentiate throughout the nervous system. Our results suggest that oligodendrocyte precursors are not simply eliminated, but instead differentiate to astrocytes. These observations are consistent with the idea that in *Olig1/2* double mutants, *Olig2*-expressing progenitors sequentially generate interneurons and astrocytes rather than motoneurons and oligodendrocytes. In this way, *Olig* genes link the specification of a particular neuronal subtype to that of a specific glial subtype, independent of the decision between neuronal versus glial fates.

Olig2 Is Required for Both the Regional Identity and Differentiation of Motoneuron Precursors

Misexpression studies in the chick have suggested that OLIG2 plays two roles in motoneuron fate determination: it specifies the regional identity of the pMN domain via repression of *Irx3*, and it promotes motoneuron progenitor cell cycle exit and differentiation, in part via local derepression of *Ngn2* (Mizuguchi et al., 2001; Novitch et al., 2001). The loss-of-function data presented in this and the companion paper (Lu et al., 2002 [this issue of *Cell*]) strengthen this view. Combined deletion of *Olig2* and *Olig1* causes a derepression of *Irx3* in pMN and a loss of *Ngn2* expression in this domain. The selective loss of *Ngn2* expression in pMN is consistent with the idea that this bHLH factor is controlled by distinct *trans*-acting factors in different progenitor domains (Scardigli et al., 2001). The motoneuron deficit in the *Olig1/2* double knockout is similar to that seen in embryos lacking *Nkx6.1/6.2* (Vallstedt et al., 2001), a homeodomain patterning molecule (Briscoe et al., 2000) that is required for *Olig2* expression (Novitch et al., 2001). The fact that expression of *Nkx6.1* and *6.2* is unperturbed in *Olig1/2* knockouts is consistent with the idea that *Olig* genes function downstream of *Nkx6.1/6.2* in motoneuron generation (Novitch et al., 2001).

Olig Genes Function Cell Autonomously in Oligodendrocyte Fate Specification

The complete failure of oligodendrocyte formation in *Olig1/2* double mutants suggests that all oligodendrocytes require *Olig* genes. Consistent with this, oligodendrocytes are not generated in neurosphere cultures derived from $Olig1^{-/-}2^{-/-}$ spinal cord (see Supplemental Figure S1 at http://www.cell.com/cgi/content/full/109/1/61/DC1). The fact that *Olig1/2* are coexpressed in oligodendrocyte precursors (this study; Lu et al., 2000; Zhou et al., 2000) suggests that this defect likely reflects a cell-autonomous requirement for these genes. An alternative explanation, however, is that this phenotype is a non-cell-autonomous consequence of the earlier loss of motoneurons, which have been hypothesized to send a feedback signal to the ventricular zone to regulate the subsequent production of oligodendrocytes (Hardy, 1997; discussed in Richardson et al., 2000).

We think this hypothesis is unlikely, however, because in $Ngn1^{-/-}$; $Ngn2^{-/-}$ double mutants, neuronal differentiation in the ventral spinal cord is largely eliminated (Scardigli et al., 2001), but oligodendrocyte precursor formation is unaffected (our unpublished observations). Similarly, in $Isl1^{-/-}$ mice which lack motoneurons (Pfaff et al., 1996), oligodendrocyte differentiation is also unaffected (Sun et al., 1998). Finally, oligodendrocytes develop normally in the hindbrain of *Olig2* single mutants (Lu et al., 2002 [this issue of *Cell*]), which lack somatic motoneurons. Our observation that in *Olig1/2* double mutants, hindbrain oligodendrocytes are completely lost further indicates that the sparing of hindbrain oligodendrocytes in $Olig2^{-/-}$ embryos is not due to compensation of a somatic motoneuron-derived signal by visceral motoneurons, which are spared in both $Olig2^{-/-}$ and $Olig1^{-/-}2^{-/-}$ mutants.

Role of *Olig* Genes in Motoneuron and Oligodendrocyte Fate Specification

The inference that *Olig* genes function cell autonomously in oligodendrocyte development leaves open the question of when that function is required. Our data indicate that both motoneurons and oligodendrocytes are normally generated from pMN (but not from p2) and support the idea (Richardson et al., 1997, 2000) that these neurons and glia share a common precursor. Consequently, the homeotic-like transformation of such pre-

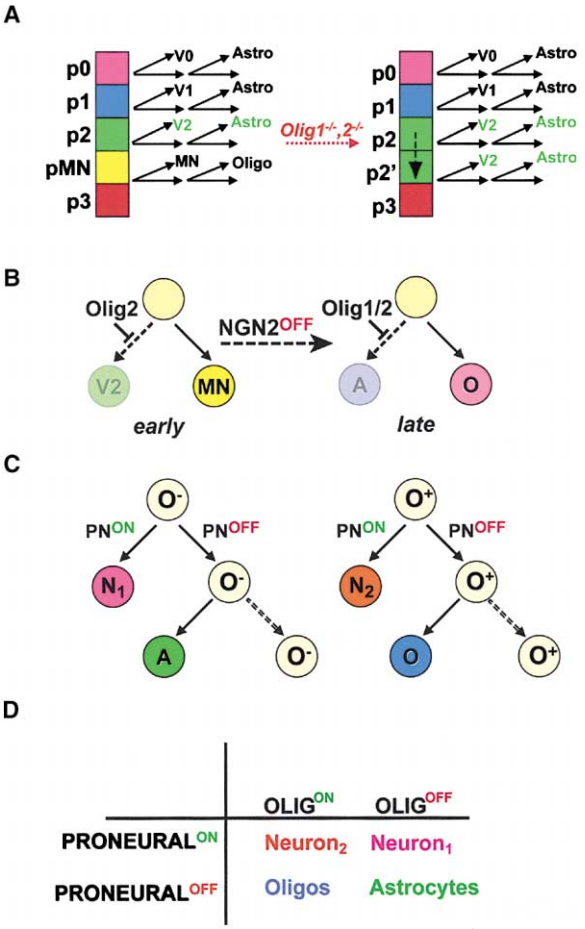

Figure 7. *Olig* Genes Control the Subtype Identities of Both Neurons and Glia Derived from a Common Progenitor Domain

(A) Summary of neuronal and glial phenotypes in *Olig1*$^{-/-}$*Olig2*$^{-/-}$ mutants.

(B) *Olig* genes may act sequentially in motoneuron (MN) and oligodendrocyte (O) development. Abbreviation: A, astrocyte.

(C) Two putative types of spinal cord progenitor cells. O^{-} progenitors do not express *Olig* genes and generate certain types of neurons (N_1) and later astrocytes (A). Abbreviation: PN, proneural. O^{+} progenitors first generate other types of neurons (N_2) and then oligodendrocytes (O, blue cell).

(D) A simple combinatorial code composed of proneural and *Olig* genes can determine whether CNS progenitors produce neurons, oligodendrocytes, or astrocytes. Neuron$_1$ and Neuron$_2$ denote two different neuronal subtypes.

cursors from a pMN to a p2 identity in *Olig1/2* homozygous embryos could result in the elimination of both cell types (Figure 7A). In that case, the wild-type function of *Olig* genes in specifying both the motoneuron and oligodendrocyte fates might simply be repression of *Irx3* in pMN. Alternatively, the mutant phenotype could reflect an independent and sequential requirement for *Olig* genes in both early patterning of the pMN domain and in oligodendrocyte fate determination (Figure 7B).

Consistent with the idea of independent functions, the hindbrain phenotype of *Olig2*$^{-/-}$ single mutants demonstrates that *Olig* gene mutations can cause deficiencies in somatic motoneuron generation without necessarily affecting oligodendrocyte development (Lu et al., 2002 [this issue of *Cell*]). Furthermore, while misexpression of *Olig2* in chick is sufficient to cause ectopic repression of *Irx3* and motoneuron induction in some regions of the spinal cord (Novitch et al., 2001), it does not induce ectopic oligodendrocyte differentiation (Zhou et al., 2001). Thus, while repression of *Irx3* by *Olig* genes may be necessary for oligodendrocyte fate determination, it may not be sufficient. Formal resolution of this issue will require selective rescue of the early pMN phase of *Olig2* expression in *Olig1/2* double knockouts to determine whether both motoneurons and oligodendrocytes are recovered.

OLIG1 and 2 Control an Oligodendrocyte versus Astrocyte Fate Choice

Our lineage-tracing data suggest that many *Olig2-hGFP*-expressing precursors generate astrocytes instead of oligodendrocytes upon deletion of *Olig1* and *Olig2*. If so, it would imply that spinal cord oligodendrocyte precursors have the potential to generate astrocytes, but that this fate is normally repressed by *Olig* genes (Figure 7B, right). Astrocytes are thought to arise from multiple levels along the dorso-ventral axis of the spinal cord (Pringle et al., 1998). Thus, it is a reasonable assumption that the p2 domain normally generates astrocytes after it generates V2 interneurons (Figure 7A, left). If so, then the trans-fating of *Olig2*-expressing progenitors to astrocytes in *Olig1/2* double mutants could reflect a conversion of progenitors that sequentially generate motoneurons and oligodendrocytes to ones that produce first V2 interneurons and then astrocytes (Figure 7A, right, p2').

If deletion of *Olig* genes causes oligodendrocyte precursors to generate astrocytes, do such precursors normally generate astrocytes following downregulation of *Olig* gene expression in the ventricular zone? We found no evidence for persistence of the OLIG2-hGFP lineage marker into astrocytes in *Olig1/2* heterozygotes. Similarly, using a permanent lineage tracer, Lu et al. (2002 [this issue of *Cell*]) found no astrocytes among the progeny of *Olig1*-expressing cells. These data suggest that *Olig*-expressing progenitors normally produce motoneurons and oligodendrocytes but not astrocytes in vivo (Figure 7C, O^{+}). This idea may seem inconsistent with the demonstration that single CNS progenitors can generate neurons, astrocytes, and oligodendrocytes in culture (reviewed in Gage, 2000; Anderson, 2001). However, despite extensive retroviral lineage tracing studies, there is no clear evidence for tripotential neuron/astrocyte/oligodendrocyte progenitors in vivo (Luskin et al., 1988; Leber et al., 1990). The tripotential CNS stem cells characterized in vitro may thus represent a more primitive progenitor than has been identified in vivo. Alternatively, the cell culture environment may reveal a combination of developmental potentials that are not actually used by any single progenitor in vivo.

The Genetic Logic of Neural Cell Fate Determination

bHLH proneural genes such as the *Ngns* control a neuron versus glial fate switch (Tomita et al., 2000; Nieto et al., 2001; Sun et al., 2001b; reviewed in Vetter, 2001). In

the case of motoneurons and oligodendrocytes, *Ngn1/2* is likely to be the proneural gene that controls this switch (this study; Mizuguchi et al., 2001; Novitch et al., 2001; Zhou et al., 2001). These data, taken together with our previous results (Zhou et al., 2001), suggest that once expression of *Ngns* has been extinguished in pMN, *Olig* genes determine whether the remaining progenitors will produce oligodendrocytes or astrocytes (Figure 7B).

These results suggest a simple combinatorial code whereby different combinations of the *Olig* and proneural genes can specify either neuronal, oligodendroglial, or astroglial fates (Figure 7D). According to this genetic logic, the astroglial fate would represent a final "ground state," in which neither proneural nor *Olig* genes are expressed. This fate may, however, require active repression by *Hes* genes, which repress proneural gene expression (Ishibashi et al., 1995; Furukawa et al., 2000; Hojo et al., 2000; Satow et al., 2001; reviewed in Fisher and Caudy, 1998).

Combinatorial codes of Lim HD and Ets domain transcription factors have been shown to control different aspects of motoneuron subtype identity (Tsuchida et al., 1994; Lin et al., 1998; Sharma et al., 1998; Kania et al., 2000). By contrast, bHLH factors have until now been viewed as primarily acting in linear cascades to produce a single cell type, such as muscle or neuron (Weintraub, 1993; Lee, 1997). The results presented here suggest that in the nervous system, bHLH factors can also function in a combinatorial code that determines the three fundamental cell types of the CNS. This code may provide a foundation upon which higher-order aspects of neuronal and glial subtype identity can be built by superimposing combinatorial codes composed of other families of transcription factors. The linking of these multiple coding systems may then be achieved by crossregulatory, and perhaps physical, interactions between the molecules that comprise them.

Experimental Procedures

Generation of Olig1 and Olig2 Double-Mutant Mice

All mouse genomic clones were derived from a 129SVJ genomic library (Stratagene). Both the mouse *Olig1* and *Olig2* sequences are encoded by a single exon. The *Olig2* targeting vector was constructed by inserting a *Histone-GFP fusion/loxp/PGKneo* cassette between a 2 kb 5′ arm and a 3.8 kb 3′ arm. For the *Olig1* targeting vector, a *tau LacZ/loxp/PGKhyg* cassette was cloned between the 1.9 kb 5′ arm and the 3.2 kb 3′ arm.

Two rounds of electroporation and selection were conducted, first with the *Olig2* targeting vector, and then with the *Olig1* targeting vector. Correctly recombined clones at both the *Olig2* and *Olig1* loci were subjected to Cre/Loxp analysis to determine whether the two recombined alleles reside on the same chromosome (protocol available upon request). The frequency of recombination for both the *Olig2* and *Olig1* loci was ~1:300. Clones in which the two mutant alleles are located in *cis* were injected into C57BL/6J blastocysts to generate germline chimeric founders. Mutant mice were genotyped with PCR primers specific to *Olig1*, *Olig2*, *GFP*, *lacZ*, *Neomycin*, and *Hygromycin* genes. No segregation of the two mutant alleles has been observed in all embryos genotyped so far. All embryos analyzed in this study were derived from heterozygous 129sv × C57BL/6J intercrosses.

In Situ Hybridization

Nonradioactive in situ hybridization was performed as previously described (Zhou et al., 2000). The following mouse gene probes were used: *Olig1*, *Olig2*, *Olig3*, *Sox10* (a gift of Dr. Kirsten Kuhlbrodt), *PDGFR*, *MBP*, *PLP/DM20*, *Ngn1*, and *Ngn3*. Probes for *Nkx6.1*, *Nkx6.2*, and *Dbx2* were the kind gift of Dr. Thomas Jessell.

Immunohistochemistry

Mouse embryos were fixed by immersion in 4% paraformaldehyde from 1 hr to overnight at 4°C depending on the age. The following primary antibodies were used: rabbit anti-Olig2 (1:2000, gift of Dr. Takebayashi Hirohide), rabbit anti-Nkx2.2 (1:1000, gift of Dr. Thomas Jessell), mAb anti-Neurogenin2 (1:100, Liching Lo), rabbit anti-Chx10 (1:4000, gift of Dr. Thomas Jessell), guinea pig anti-Irx3 (1:1000, gift of Dr. Thomas Jessell), rabbit anti-Hb9 (1:2000, gift of Dr. Samuel Pfaff), rabbit anti-GFP and Alexa-488 conjugated rabbit anti-GFP (1:1000, Molecular Probes), rabbit anti β-gal (1:1000, 5′-3′), rabbit anti-GFAP (1:1000, DAKO), mAb anti-S100 β (1:1000, Sigma), and rabbit anti-Phox2b (1:700, gift of Dr. Jean-Francois Brunet). mAbs against Lim3, MNR2/Hb9, Engrailed-1, Isl1/2, Hb9, Lim3, Nkx2.2, and Pax6 were obtained from Developmental Studies Hybridoma Bank (DSHB). Whole-mount antibody staining of mouse embryos was performed as described previously (Ma et al., 1996).

BrdU Labeling and TUNEL Assay

BrdU labeling of mouse embryos was conducted by intraperitoneal injection of BrdU (Sigma, 65 mg/g body weight) 2 hr before sacrifice. A rat anti-BrdU antibody (Accurate) was used to detect BrdU. TUNEL assays were performed with a kit from Roche according to the manufacturer's instructions.

Acknowledgments

We thank Drs. Richard Lu, Charles Stiles, and David Rowitch for communicating unpublished results and Tom Jessell for advice, reagents, helpful discussions, and critical comments on the manuscript. We are also grateful to Shirley Peace and Bruce Kennedy of the Caltech Transgenic Facility, Joana Yamada for technical assistance, and Gaby Mosconi for laboratory management. This work was supported by National Institutes of Health Grant RO1-NS23476. D.J.A. is an Investigator of the Howard Hughes Medical Institute.

Received: November 28, 2001
Revised: February 13, 2002
Published online: March 11, 2002

References

Anderson, D.J. (2001). Stem cells and pattern formation in the nervous system: the possible versus the actual. Neuron *30*, 19–35.

Briscoe, J., Sussel, L., Serup, P., Hartigan-O'Connor, D., Jessell, T.M., Rubenstein, J., and Ericson, J. (1999). Homeobox gene Nkx2.2 and specification of neuronal identity by graded Sonic hedgehog signalling. Nature *398*, 622–627.

Briscoe, J., Pierani, A., Jessell, T.M., and Ericson, J. (2000). A homeodomain protein code specifies progenitor cell identity and neuronal fate in the ventral neural tube. Cell *101*, 435–445.

Dubreuil, V., Hirsch, M., Pattyn, A., Brunet, J., and Goridis, C. (2000). The Phox2b transcription factor coordinately regulates neuronal cell cycle exit and identity. Development *127*, 5191–5201.

Farah, M.H., Olson, J.M., Sucic, H.B., Hume, R.I., Tapscott, S.J., and Turner, D.L. (2000). Generation of neurons by transient expression of neural bHLH proteins in mammalian cells. Development *127*, 693–702.

Fisher, A., and Caudy, M. (1998). The function of hairy-related bHLH repressor proteins in cell fate decisions. Bioessays *20*, 298–306.

Furukawa, T., Mukherjee, S., Bao, Z.Z., Morrow, E.M., and Cepko, C.L. (2000). rax, Hes1, and notch1 promote the formation of Muller glia by postnatal retinal progenitor cells. Neuron *26*, 383–394.

Gage, F. (2000). Mammalian neural stem cells. Science *287*, 1433–1438.

Gradwohl, G., Fode, C., and Guillemot, F. (1996). Restricted expression of a novel murine *atonal*-related bHLH protein in undifferentiated neural precursors. Dev. Biol. *180*, 227–241.

Hall, A., Giese, N.A., and Richardson, W.D. (1996). Spinal cord oligo-

dendrocytes develop from ventrally derived progenitor cells that express PDGF alpha-receptors. Development *122*, 4085–4094.

Hardy, R.J. (1997). Dorsoventral patterning and oligodendroglial specification in the developing central nervous system. J. Neurosci. Res. *50*, 139–145.

Hojo, M., Ohtsuka, T., Hashimoto, N., Gradwohl, G., Guillemot, F., and Kageyama, R. (2000). Glial cell fate specification modulated by the bHLH gene Hes5 in mouse retina. Development *127*, 2515–2522.

Ishibashi, M., Ang, S.-L., Shiota, K., Nakanishi, S., Kageyama, R., and Guillemot, F. (1995). Targeted disruption of mammalian *hairy* and *Enhancer of split* homolog-1 (*HES-1*) leads to up-regulation of neural helix-loop-helix factors, premature neurogenesis, and severe neural tube defects. Genes Dev. *9*, 3136–3148.

Jessell, T.M. (2000). Neuronal specification in the spinal cord: inductive signals and transcriptional codes. Nat. Rev. Genet. *1*, 20–29.

Johnson, J.E., Birren, S.J., and Anderson, D.J. (1990). Two rat homologues of *Drosophila achaete-scute* specifically expressed in neuronal precursors. Nature *346*, 858–861.

Kanda, T., Sullilvan, K.F., and Wahl, G.M. (1998). Histon-GFP fusion protein enables sensitive analysis of chromosome dynamics in living mammalian cells. Curr. Biol. *8*, 377–385.

Kania, A., Johnson, R., and Jessell, T. (2000). Coordinate roles for Lim homeobox genes in directing the dorsoventral trajectory of motor axons in the vertebrate limb. Neuron *102*, 161–173.

Leber, S.M., Breedlove, S.M., and Sanes, J.R. (1990). Lineage, arrangement, and death of clonally related motorneurons in chick spinal cord. J. Neurosci. *10*, 2451–2462.

Lee, J.E. (1997). Basic helix-loop-helix genes in neural development. Curr. Opin. Neurobiol. *7*, 13–20.

Lin, J.H., Saito, T., Anderson, D.J., Lance-Jones, C., Jessell, T.M., and Arber, S. (1998). Functionally-related motor neuron pool and muscle sensory afferent subtypes defined by coordinate *ETS* gene expression. Cell *95*, 393–407.

Lo, L., Dormand, E., Greenwood, A., and Anderson, D.J. (2002). Comparison of the generic neuronal differentiation and neuron subtype specification functions of mammalian *achaete-scute* and *atonal* homologs in cultured neural progenitor cells. Development, in press.

Lu, Q.R., Yuk, D., Alberta, J.A., Zhu, Z., Pawlitzky, I., Chan, J., McMahon, A.P., Stiles, C.D., and Rowitch, D.H. (2000). Sonic hedgehog-regulated oligodendrocyte lineage genes encoding bHLH proteins in the mammalian central nervous system. Neuron *25*, 317–329.

Lu, Q.R., Cai, L., Rowitch, D., Cepko, C.L., and Stiles, C.D. (2001). Ectopic expression of Olig1 promotes oligodendrocyte formation and reduces neuronal survival in developing mouse cortex. Nat. Neurosci. *4*, 973–974.

Lu, Q.R., Sun, T.S., Zhu, Z., Ma, N., Garcia, M., Stiles, C.D., and Rowitch, D.H. (2002). Common developmental requirement for *Olig* function indicates a motor neuron/oligodendrocyte connection. Cell *109*, in press, 61–73.

Luskin, M.B., Pearlman, A.L., and Sanes, J.R. (1988). Cell lineage in the cerebral cortex of the mouse studied in vivo and in vitro with a recombinant retrovirus. Neuron *1*, 635–647.

Ma, Q., Kintner, C., and Anderson, D.J. (1996). Identification of *neurogenin*, a vertebrate neuronal determination gene. Cell *87*, 43–52.

McCormick, M.B., Tamimi, R.M., Snider, L., Asakura, A., Bergstrom, D., and Tapscott, S.J. (1996). *neuroD2* and *neuroD3*: distinct expression patterns and transcriptional activation potentials within the *neuroD* gene family. Mol. Cell. Biol. *16*, 5792–5800.

Miller, R. (1996). Oligodendrocyte origins. Trends Neurosci. *19*, 92–96.

Mizuguchi, R., Sugimori, M., Takebayashi, H., Kosako, H., Nagao, M., Yoshida, S., Nabeshima, Y., Shimamura, K., and Nakafuku, M. (2001). Combinatorial roles of olig2 and neurogenin2 in the coordinated induction of pan-neuronal and subtype-specific properties of motoneurons. Neuron *31*, 757–771.

Muhr, J., Anderson, E., Persson, M., Jessell, T., and Ericson, J. (2001). Groucho-mediated transcriptional repression establishes progenitor cell pattern and neuronal fate in the vertral neural tube. Cell *104*, 861–873.

Nieto, M., Schurmans, C., Britz, O., and Guillemot, F. (2001). Neural bHLH genes control the neuronal versus glial fate decision in cortical progenitors. Neuron *29*, 401–413.

Novitch, B.G., Chen, A.I., and Jessell, T.M. (2001). Coordinate regulation of motor neuron subtype identity and pan-neuronal properties by the bHLH repressor Olig2. Neuron *31*, 773–789.

Parras, C.M., Schuurmans, C., Scardigli, R., Kim, J., Anderson, D.J., and Guillemot, F. (2002). Divergent functions of the proneural genes *Mash1* and *Ngn2* in the specification of neuronal subtype identity. Genes Dev. *16*, 324–338.

Pfaff, S.L., Mendelsohn, M., Stewart, C.L., Edlund, T., and Jessell, T.M. (1996). Requirement for LIM homeobox gene *Isl1* in motor-neuron generation reveals a motor neuron-dependent step in interneuron differentiation. Cell *84*, 309–320.

Pringle, N.P., Guthrie, S., Lumsden, A., and Richardson, W.D. (1998). Dorsal spinal cord neuroepithelium generates astrocytes but not oligodendrocytes. Neuron *20*, 883–893.

Raff, M.C. (1989). Glial cell diversification in the rat optic nerve. Science *243*, 1450–1455.

Richardson, W.D., Pringle, N.P., Yu, W.-P., and Hall, A.C. (1997). Origins of spinal cord oligodendrocytes: possible developmental and evolutionary relationships with motor neurons. Dev. Neurosci. *19*, 58–68.

Richardson, W.D., Smith, H.K., Sun, T., Pringle, N.P., Hall, A., and Woodruff, R. (2000). Oligodendrocyte lineage and the motor neuron connection. Glia *29*, 136–142.

Satow, T., Bae, S., Inoue, T., Inoue, C., Miyoshi, G., Tomita, K., Bessho, Y., Hashimoto, N., and Kageyama, R. (2001). The basic Helix-Loop-Helix gene Hesr2 promotes gliogenesis in mouse retina. J. Neurosci. *21*, 1265–1273.

Scardigli, R., Schuurmans, C., Gradwohl, G., and Guillemot, F. (2001). Crossregulation between *Neurogenin2* and pathways specifying neuronal identity in the spinal cord. Neuron *31*, 203–217.

Sharma, K., Sheng, H.Z., Lettieri, K., Li, H., Karavanat, A., Potter, S., Westphal, H., and Pfaff, S.L. (1998). LIM homeodomain factors Lhx3 and Lhx4 assign subtype identities for motor neurons. Cell *95*, 817–828.

Sun, T., Pringle, N., Hardy, A.P., Richardson, W.D., and Smith, H.K. (1998). Pax6 influences the time and site of origin of glial precursors in the ventral neural tube. Mol. Cell. Neurosci. *12*, 228–239.

Sun, T., Echelard, Y., Lu, R., Yuk, D., Kaing, S., Stiles, C.D., and Rowitch, D.H. (2001a). Olig bHLH proteins interact with homeodomain proteins to regulate cell fate acquisition in progenitors of the ventral neural tube. Curr. Biol. *11*, 1413–1420.

Sun, Y., Nadal-Vincens, M., Misono, S., Lin, M.Z., Zubiaga, A., Hua, X., Fan, G., and Greenberg, M.E. (2001b). Neurogenin promotes neurogenesis and inhibits glial differentiation by independent mechanisms. Cell *104*, 365–376.

Takebayashi, H., Yoshida, S., Sugimori, M., Kosako, H., Kominami, R., Nakafuku, M., and Nabeshima, Y. (2000). Dynamic expression of basic helix-loop-helix Olig family members: implication of Olig2 in neuron and oligodendrocyte differentiation and identification of a new member, Olig3. Mech. Dev. *99*, 143–148.

Tomita, K., Moriyoshi, K., Nakanishi, S., Guillemot, F., and Kageyama, R. (2000). Mammalian achaete-scute and atonal homologs regulate neuronal versus glial fate determination in the central nervous system. EMBO J. *19*, 5460–5472.

Tsuchida, T., Ensini, M., Morton, S.B., Baldassare, M., Edlund, T., Jessell, T.M., and Pfaff, S.L. (1994). Topographic organization of embryonic motor neurons defined by expression of LIM homeobox genes. Cell *79*, 957–970.

Vallstedt, A., Muhr, J., Pattyn, A., Pierani, A., Mendelsohn, M., Sander, M., Jessell, T.M., and Ericson, J. (2001). Different levels of repressor activity assign redundant and specific roles to Nkx6 genes in motor neuron and interneuron specification. Neuron *31*, 743–755.

Vetter, M. (2001). A turn of the helix: preventing the glial fate. Neuron *29*, 559–562.

Weintraub, H. (1993). The MyoD family and myogenesis: redundancy, networks and thresholds. Cell *75*, 1241–1244.

Woodruff, R.H., Tekki-Kessaris, N., Stiles, C.D., Rowitch, D.H., and Richardson, W.D. (2001). Oligodendrocyte development in the spinal cord and telencephalon: common themes and new perspectives. Int. J. Dev. Neurosci. *19*, 379–385.

Zhou, Q., Wang, S., and Anderson, D.J. (2000). Identification of a novel family of oligodendrocyte lineage-specific basic helix-loop-helix transcription factors. Neuron *25*, 331–343.

Zhou, Q., Choi, G., and Anderson, D.J. (2001). The bHLH transcription factor Olig2 promotes oligodendrocyte differentiation in collaboration with Nkx2.2. Neuron *31*, 791–807.